Probe Report

Probe project: Selective GPR35 Antagonists
Title: Antagonists for the Orphan Receptor GPR35
Authors: Susanne Heynen-Genel, Russell Dahl, Shenghua Shi, Michelle Sauer, Santosh Hariharan, Eduard Sergienko, Shakeela Dad, Thomas Chung, Derek Stonich, Ying Su, Pingwei Zhao, Marc G. Caron, Mary E. Abood and Lawrence S. Barak
Assigned Assay Grant #: 1 X01 MH085708-01
Screening Center Name & PI: Sanford-Burnham Center for Chemical Genomics (*NIH PubChem & MLPCN designation*) & John C. Reed
Chemistry Center Name & PI: Burnham Center for Chemical Genomics & John C. Reed **Assay Submitter & Institution:** Lawrence S. Barak, Duke University Medical Center
Collaborating PI: (Mary E. Abood, Temple University, PA)

PubChem Summary Bioassay Identifier (AID): 2079

Abstract: Although many known receptors that regulate addiction have been pharmacologically and biochemically well characterized, some orphan receptors with homology to known receptors of abuse (i.e. GPR35) remain uncharacterized. GPR35 is a G-protein coupled receptor, first identified in 1998 after a screen of a human genomic library. More recent RT-PCR studies have now confirmed the presence of GPR35 in dorsal root ganglion, the cerebellum and brain, as well as GPR35b, which was cloned from a human whole brain cDNA library. Thus, GPR35 regulation appears to have profound physiological and pathophysiological implications. We have identified a 3rd antagonist, **ML194** that represents a different chemical scaffold with potency (160 nM) and selectivity (>57-fold) for GPR35, but not for the related GPR55 orphan receptor, that is intermediate between the previously reported probes, ML145 (CID2286812) and ML144 (CID1542103). **ML194** also does not seem to produce non-specific interference with signaling directly at or downstream of the β-arrestin signaling pathway, so it may serve as an additional tool to delineate the biochemistry of GPR35 as potential therapeutics to selectively target pathways underlying pain and to enhance our understanding of the molecular basis of addiction.

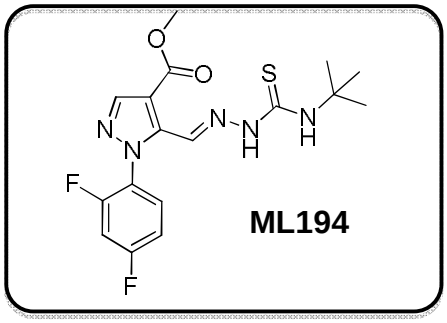

Probe(s) Structure & Characteristics:
This Center Probe Report describes a third selective antagonist for GPR35, an orphan GPCR receptor, that represent a novel scaffold or chemical series: (3) CID9581011. Two probes from other scaffolds were reported in a previous probe report "Antagonists for the Orphan Receptor GPR35" (http://www.ncbi.nlm.nih.gov/books/NBK50703/)

CID**	Target Name	IC_{50}/EC_{50} (nM) [SID, AID]	Anti-target Name(s)	IC_{50}/EC_{50} (μM) [SID, AID]	Selectivity	Secondary Assay(s) Name: IC_{50}/EC_{50} (nM) [SID, AID]
9581011 *(scaffold3)* **ML194**	GPR35 Antagonist *Orphan GPCR receptor*	160 nM SID99309109 AID463227	GPR55 Antagonist *Orphan GPCR receptor*	~ 9.08 μM SID99309109 AID463228	~57-fold vs. GPR55 Antagonist	N/A

Recommendations for the scientific use of this probe:

Many receptors regulating addiction are pharmacologically and biochemically well characterized, but some orphan receptors like GPR35 with homology to known receptors of abuse remain uncharacterized. The aim of this research is to identify small molecule antagonists of human GPR35.The identification of small molecules capable of selectively inhibiting or activating orphans will provide tools for elucidating novel molecular pathways underlying addictive behaviors. These novel compounds will then be utilized to elucidate a number of things such as characterize GPR35 biology in vitro, GPR35 in animal models of pain and enhance the understanding of the molecular basis of addiction.

1. Scientific Rationale for Project

Drug addiction continues to remain a major public health concern in the United States. Addictive behavior results from changes in central nervous system signaling pathways that are modified after exposure to drugs of abuse. In particular, compounds such as cannabinoids and opiates that influence mood and pain perception are commonly associated with addictive behaviors. Many receptors regulating addiction are pharmacologically and biochemically well characterized, but some orphan receptors like GPR35 with homology to known receptors of abuse remain almost totally uncharacterized. GPR35 is a G-protein coupled receptor that was first identified in 1998 after a screen of a human genomic library (1). GPR35 is homologous to P2Y purinergic receptors and GPR23, whose ligand is lysophosphatidic acid. GPR35 shares a 30 percent identity with the putative cannabinoid receptor GPR55 (2-5). The ability of GPR55 to recognize cannabinoids was first described in a yeast expression system, where the CB1 antagonists AM251 and SR141716A (rimonabant) acted as agonists (6). Preliminary studies of GPR35 by mRNA expression showed it expressed predominantly in the immune and gastrointestinal systems (1). However, recent RT-PCR studies have confirmed the presence of GPR35 in dorsal root ganglion, the cerebellum and brain, and GPR35b was cloned from a human whole brain cDNA library (2, 5, 7). Variable Gi/o protein activation by GPR35 that was pertussis toxin sensitive was subsequently observed in rat sympathetic neurons (2).

There are approximately fifteen papers characterizing GPR35 in the PubMed listed peer reviewed literature. An N-terminal splice variant of GPR35, GPR35b, was identified from a genetic screen of gastric carcinomas (8), leading to speculation that GPR35 regulates cell growth. The observation that the *a* isoform possessed a stronger transforming activity than the *b* also led the authors to postulate that GPR35a possesses constitutive activity (8). While GPR35 has been implicated in the formation of gastric cancers (8), conversely, deletion of GPR35 may be responsible for a mental retardation syndrome associated with deletions on 2q37.3 (9). There are no reports in the peer reviewed literature (PubMed) of GPR35 antagonists other than from our recent publication (Zhao *et al.* Mol Pharmacol. 2010 Oct; **78**(4):560-8. Epub 2010 Jul 22.) that includes results from this GPR35 antagonist screen. A recent SciFinder search on March 28, 2011 did not uncover any novel matter than those disclosed by the prior and this MLP probe report.

GPR35 regulation appears to have profound physiological and pathophysiological implications so that defining compounds that regulate GPR35 will be important. The specific aim of this grant is to identify small molecule antagonists of human GPR35. These novel compounds will be utilized to characterize GPR35 biology in vitro and GPR35 in animal models of pain. Thus, this proposal will provide tools for delineating the biochemistry of GPR35, potentially provide compounds for targeted therapeutics of pathways underlying pain, and enhance our understanding of the molecular basis of addiction.

2. Project Description

The goal of the high-throughput screen (HTS) was to identify novel and specific inhibitors of GPR35. To date, no antagonists for GPR35 are known and the goal of this project was to identify small molecules that had an IC50 of 5μM or less in the primary GPR35 β-arrestin HCS assay, with at least 10-fold antagonist selectivity against the related receptor GPR55.

Table 1. Assays for GPR35					
PubChem BioAssay Name	**AIDs**	**Probe Type**	**Assay Type**	**Assay Format**	**Assay Detection (well format)**
Summary of Image-based HTS for Selective Antagonists of GPR35	2079	Antagonists	Summary	N/A	N/A
Image-Based HTS for Selective Antagonists of GPR35 [Primary]	2058	Antagonists	Primary	Cell-based	Imaging method (384)
HCS GPR35 Antagonist SAR-primary assay used as secondary	2480, 463227	Antagonists	SAR	Cell-based	Imaging method (384)
HCS GPR55 antagonist – Counterscreen - SAR	2397, 463228	Antagonists	SAR	Cell-based	Imaging method (384)

Primary Screen

This image-based high-content screen (HCS) is based on fluorescence redistribution of a GFP-β-arrestin complex from homogeneous distribution in the cytoplasm via the plasma membrane to intracellular pits and vesicles (assay technology marketed as Transfluor® assay by Molecular Devices). Upon activation by ligand binding, GPCRs undergo deactivation or "desensitization" by binding of the β-arrestin protein to the activated receptor. The GPCR-β-arrestin complex internalizes, the ligand is removed and the receptor is recycled back to the cell membrane (**Figure 1**). Localization of the fluorescently labeled β-arrestin can be monitored by image analysis (10). The primary screen assay is designed to identify compounds inhibiting GPR35 signaling induced by the GPR35 agonist Zaprinast at an approximately EC80 concentration (5). We utilize stable cell lines generated by Dr. Abood and Dr. Barak's laboratories, which performed similarly in transient transfections with the GPCR-β-arrestin tagged constructs. Dr. Abood's laboratory confirmed that the untagged human and mouse GPR35 receptors respond similarly to the tagged receptors (12).

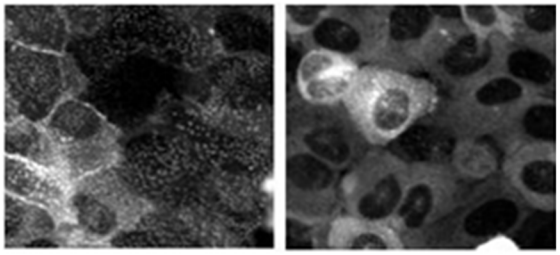

Figure 1. GPR35 Example Images of Positive and Negative Controls: Effect of 10 μM agonist Zaprinast (left panel) compared to DMSO control (right panel).

Primary Assay Materials:

Table 2. Critical Reagents used for the uHTS experiments	
Reagent	**Vendor**
U2OS (Human Osteosarcoma) cell line stably expressing GFP-tagged β-arrestin & over-expressing the GPR35 receptor	Cells from AP, scaled-up by BCCG
Zaprinast - GPR35 Agonist	ALEXIS Biochemicals (now Enzo Life Sciences)
Paraformaldehyde - Fixative	ACROS Organics
DAPI – Nuclei Stain	Invitrogen

Primary Screen Protocol:

A. Plate Preparation:

1) 45μl of cell suspension (133,000 cells/ml in culture medium) was dispensed in each well of the assay plates using a Wellmate bulk dispenser.
2) Plates were incubated overnight or approximately 20 hours at 37 degree C and 5% CO2.
3) Serum was removed by media aspiration and replaced with 45μl serum-free MEM prior to addition of compounds.
4) Compound addition was done on a Biomek FX with 384-head dispenser (Beckman):
   a) 5μl of 100μM compound solution was added to columns 3 through 24 of the assay plates for a final assay compound concentration of 10μM and 0.5% DMSO.
   b) 5μl of 5% DMSO was added to columns 1 and 2 to balance the volume and DMSO concentration across the plate.
   c) 5μl of positive control (2% DMSO) working solution was added to column 1.

5) Plates were incubated for 15 minutes at room temperature.
6) Agonist addition was done on a Biomek FX with 384-head dispenser (Beckman). 5µl of agonist (100µM Zaprinast) working solution was added to columns 2-24. (This also serves as the negative control in column 2.)
7) Plates were incubated for 45 minutes at 37 degrees C and 5% CO2.
8) Media was aspirated leaving 20µl liquid in each well using a Titertek plate washer.
9) 40µl of fixative working solution was added to each well using a Wellmate bulk dispenser (Matrix) for a final concentration of 4% PFA.
10) Plates were incubated for 40 minutes at room temperature.
11) Fixative was aspirated and plates were washed twice with 50µl PBS leaving 20µl liquid in each well using a Titertek plate washer.
12) 40µl of DAPI working solution was added using a Wellmate bulk dispenser for a final DAPI concentration of 100ng/ml. Aluminum plate seals were applied to each plate.

B. Image Acquisition and Analysis:
1) Image acquisition was performed on an Opera QEHS (Perkin Elmer) with 45 plate capacity loader/stacker and the following settings:
- 40x 0.6 NA air objective
- Acquisition camera set to 2-by-2 binning for an image size of 688 by 512 pixels
- 2 channels acquired sequentially: Exp1Cam1 = B-arrestin GFP using 488 nm laser excitation and 540/70 nm 4mission filters, Exp2Cam2 = DAPI (nuclei) using 365 nm Xenon lamp excitation and 450/50 nm emission filters
- 3 fields per well

2) Image analysis was performed using the Acapella™ Spot Detection Algorithm with the following analysis settings:

NUCLEI DETECTION	
- Threshold Adjustment:	4
- Nuclear Splitting Adjustment:	10
- Individual Threshold Adjustment	0.05
- Minimum Nuclear Area:	200
- Minimum Nuclear Contrast:	0
CYTOPLASM DETECTION	
- Cytoplasm Individual Threshold Adjustment:	0
SPOT DETECTION	
- Spot Minimum Distance	3
- Spot Peak Radius	0
- Spot Reference Radius	3
- Spot Minimum Contrast	0.26
- Spot Minimum to Cell Intensity	0.5

3) Metrics calculated from…
NUCLEI IMAGES: Cell Count (“NumberofCellsAnalyzed”), Nuclei Area (“AreaoftheNucleus”), Integrated Intensity of the Nuclei (“TotalIntegratedIntensityoftheNucleus”), Average Intensity of the Nuclei (“AverageIntensityoftheNucleus”)
GFP IMAGES: Integrated Intensity of the Cytoplasm (“TotalCytoplasmIntensity”), Integrated Intensity of the Detected Spots (“TotalSpotIntensity”), Ratio of the Integrated Spot to Integrated Cytoplasm Intensities (“RatioofSpotIntensitytoCytoplasmintensity”), Number of Spots per Cell (“AverageSpotsPerCell”)

The primary screen was performed at a compound concentration of 10 µM in 384-well format. The average Z’ for the screen was 0.65 and Z’ values ranged from 0.44 to 0.82 using the ratio of the GFP intensity of the spots over the GFP intensity of the cytoplasm (“RatioofSpotIntensitytoCytoplasmintensity”) as the primary assay read-out.

Rationale for confirmatory, counter and selectivity assay See flowchart below:

Confirmation Assays

Initial hit confirmation of compound solutions resupplied by the MLSMR was done at a single compound concentration (10µM) in duplicates using the primary screen assay to confirm activity of the hit compounds. Compounds with confirmed activity at 10 µM were tested from stock solutions resupplied by the MLSMR in 7-point dose responses (0.5 to 32µM) to evaluate potency. Potent

compounds (IC50 <5µM) were clustered into scaffolds and 10-point dose responses (0.06 to 32µM) were performed for dry powder compounds selected from hits and their commercially available analogs.

Counterscreen / Selectivity Assays

To eliminate artifacts introduced by the β-arrestin-GFP assay technology, an image-based high-content assay using the same assay technology was performed against the putative cannabinoid receptor GPR55 in antagonist mode. In addition to eliminating false positives caused by assay artifacts, this assay also evaluates selectivity of the GPR35 hit compounds against the GPR55 receptor. This is of additional interest since GPR35 and GPR55 share ~30% identity (2-5). In addition, GFP intensity of the cells was quantified to identify compounds causing cellular fluorescence resulting in a decrease in number of detected spots and thus false positive results.

Secondary Probe Characterization Assays

The identified GPR35 antagonist probes are characterized further by an assay performed in the Dr. Barak's and his collaborator's labs. This assay evaluates ERK1/2 activity downstream in the GPR35 signaling pathway.

3. Center Summary of Results

The GPR35 antagonist primary screen of 291,994 compounds resulted in 549 compounds that were considered as hits using the hit criteria of >50% activity as compared to cells without agonist addition, >30 cells in the imaged area of the well, and a total GFP intensity of <10,000,000 relative units. The upper limit for the total GFP intensity was added as hit criterion to eliminate cell-permeable autofluorescent compounds interfering with detection of spot formation.

Stock solutions resupplied by the MLSMR of 490 compounds were tested for hit confirmation. Single point confirmations at 10µM concentration were conducted in duplicate on these compounds. 102 of these compounds confirmed using the same hit criteria as for the primary screening campaign. Further testing of these compounds using a seven-point dose response (0.5 to 32µM concentration range) identified 33 compounds with an IC50 of less than 1µM and 57 compounds with an IC50 between 1 and 10µM.

The hits were clustered into scaffolds by using a maximum-common-substructure-based algorithm. Analyzing the assay data in terms of scaffolds therefore, yielded 22 hits from 8 scaffolds and 38 of their commercially available analogs were selected for dry powder purchase. Testing of these dry powder compounds in 10-point dose responses using the primary screen assay and the GPR55 antagonist counterscreen/ selectivity assay resulted in 26 compounds with IC50 < 5µM and GPR55 antagonist selectivity of IC50 (GPR55) > 10x IC50 (GPR35) spanning 5 scaffolds (**Figure 2**). Probes resulting from these scaffolds were published in a separate probe report. 14 compounds and analogs from an additional scaffold of interest to Dr. Barak and his collaborators were also ordered and tested in dose responses using the primary screen assay and the GPR55 antagonist selectivity assay. 10 of these compounds resulted in IC50 < 5µM and all of these were selective against GPR55 Antagonist (See "Round 2" in SAR section of **Figure 2**).

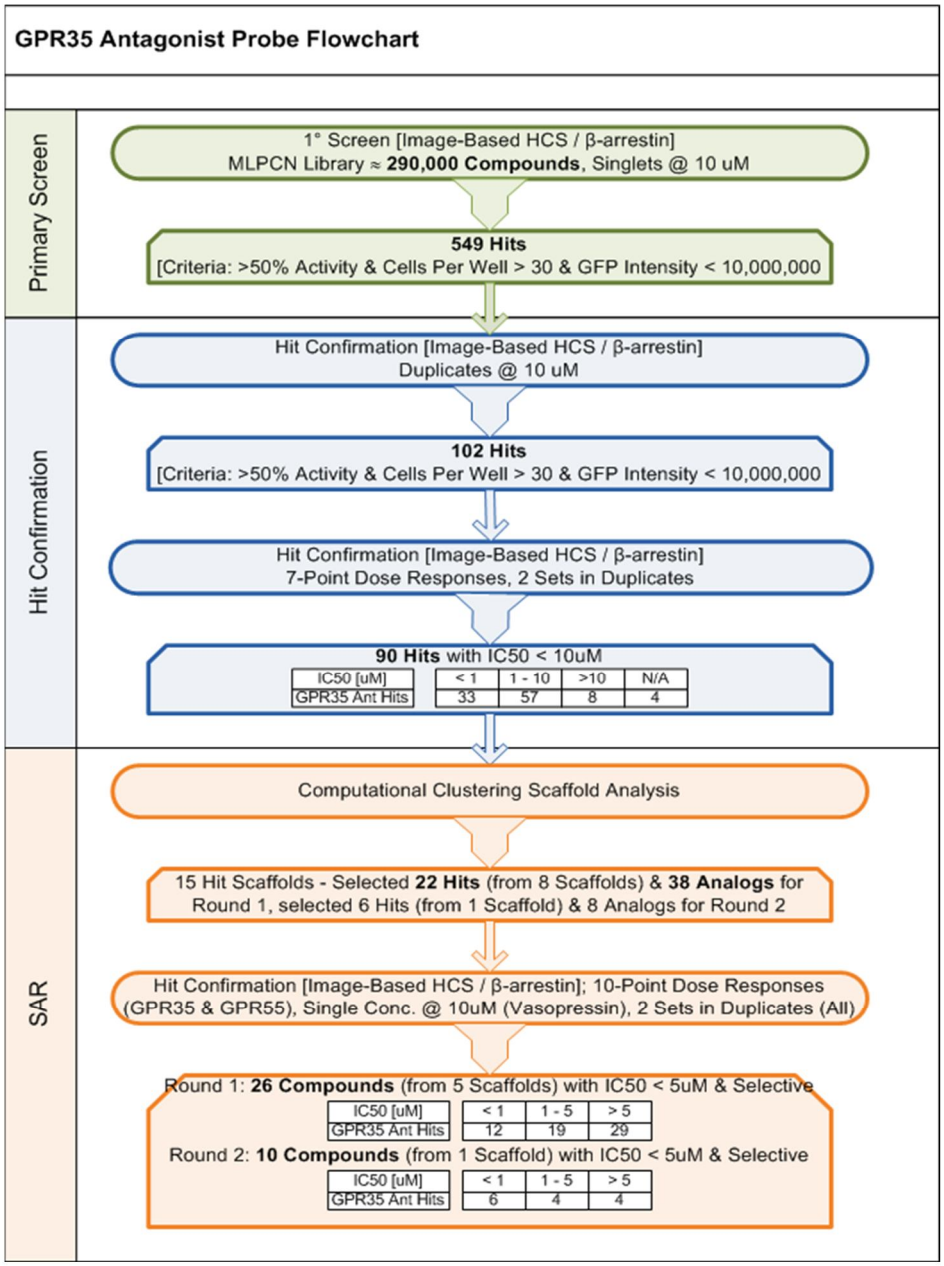

Figure 2. The GPR35 Antagonist Probe Flowchart summarizes the compound triage and decision tree for advancement of the compounds.

We note that the CID and SID of the actual nominated solid sample of the probe and some of the analogs are different than the solutions that were tested during hit validation and primary screening. This is due to the solution sample having an indeterminate double bond stereochemistry around the imine moiety ("X-crossed bond representation) in the original CID enumeration

CID9581011
SID99309109
MLS-0300303

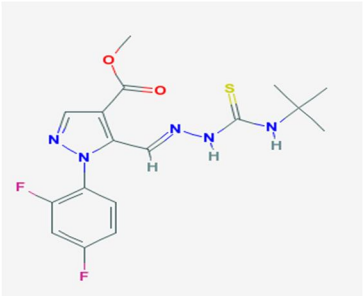

CID2745687
SID26730533
MLS-0396531
(indeterminate)

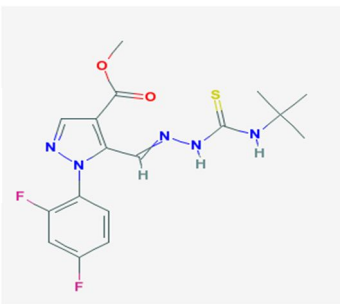

Table 3: SAR for GPR35 Antagonist ML194 (3rd probe)							
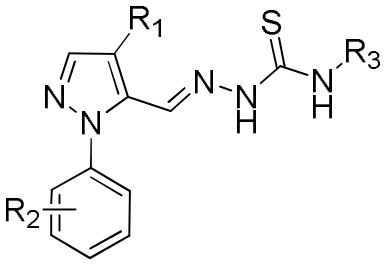			PubChem SID	PubChem CD	GPR35 Antagonist	GPR55 Antagonist	
R_1	R_2	R_3			Average IC50 ± S.E.M. (μM) (*n = 3) replicates unless otherwise indicated*		Purchased Analog (P) or Hit
COOMe **ML194**	2,4-di-F	*t*-Bu	99309109	9581011	0.160 ± 0.013	9.11 ± 1.6 *(n = 2)*	Hit
COOMe	2,4-di-F	4-Cl-Ph	99309108	9581010	0.171 ± 0.021	>32	P
COOMe	4-Cl	Ph	99309113	9581015	0.211 ± 0.019	>32	P
COOMe	H	*t*-Bu	99309103	9581005	0.307 ± 0.141	6.58 ± 0.49 *(n = 2)*	P
COOMe	H	4-Cl-Ph	99309105	9581007	0.319 ± 0.063	>32	Hit
COOMe	2,4-di-F	Ph	99309110	9581012	0.379 ± 0.057	>32	P
COOMe	H	Ph	99309104	9581006	1.02 ±0.13	15.1	Hit
COOMe	4-Cl	Me	99309111	9581013	1.25 ±0.21	>32	P
COOMe	2,4-di-F	Me	99309106	9581008	2.49 ±0.42	>32	Hit
COOMe	4-Cl	H	99309112	9581014	4.61 ±1.32	>32	Hit
COOMe	H	H	99309114	9581004	>32	>32	P
COOMe	2,4-di-F	H	99309107	9581009	>32	>32	hit
H	H	H	99309115	5335766	>32	>32	P
H	4-OMe	*t*-Bu	99309102	5703674	>32	16.4 *(n = 1)*	P

The SAR around the probe molecule **ML194** can be seen in **Table 3**. This class consists of pyrazole core and a functionalized hydrazonourea moiety. The pyrazole contains either an ester or hydrogen function at the 4 position on the ring (R_1), a phenyl ring at the 1 position, substituted with an R_2 group, and a terminally substituted hydrozonourea at the pyrazole 5 position (R_3). As seen in the SAR table (**Table 3**), there is a requirement that R_1 must be an ester group. Replacement of this group by H, as in CIDs 5335766 and 5703674, results in all GPR35 antagonism being lost, regardless of R_2 or R_3 substitution. After establishing this required R_1 functionality, substitution at R_2 was explored. While unsubstituted phenyl did indeed produce potent GPR35 antagonists, exemplified by CID 9581005, this compound also displayed off target antagonism of GPR55. Thus,

substitution on this phenyl was pursued to attempt to impart additional selectivity. It was found that o*rtho* and *para* substitution was preferred. In fact, the 2,4-fluoro analogues were very potent (CIDs 9581011 and 9581010) and selective. Derivatives with 4-chloro substitution also gave potent IC_{50} values. Finally, R_3 was explored with both aromatic and alkyl substituents. It is clear that there are preferred groups at this position, specifically *tert*-butyl, phenyl, or 4-chloro-phenyl. Finally, substitution with H at R_3 yielded only one weakly active GPR35 antagonist, CID 9581014.

4. Probe(s)

a. **Chemical name of probe compound (s)** The IUPAC name of probe the probe **ML194** is methyl 5-((2-(tert-butylcarbamoyl)hydrazono)methyl)-1-(2,4-difluorophenyl)-1*H*-pyrazole-4-carboxylate

b. Probe chem*i*cal structure(s) including stereochemistry if known

The probe **ML194** has no chiral centers (See **Fig. 3**)

Figure 3. Structure of Probe **ML194**

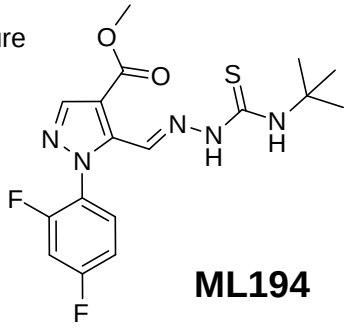

Structural Verification Information of probe (SID99309109)

c. The compound batch (substance) submitted to the MLSMR is archived as SID99309109 corresponding to CID9581011 - please see **Fig. 4(a-c)** below for the relevant spectra.

Figure 4a. ^{1}H-NMR spectrum of **ML194**

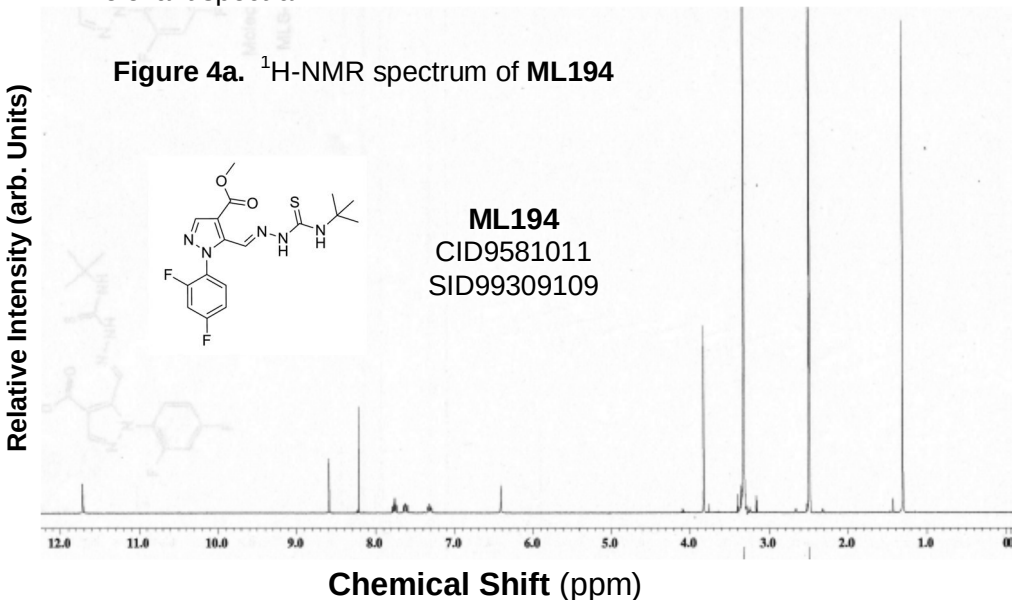

Figure 4b. Reverse-Phase High Performance Liquid Chromatogram of **ML194**

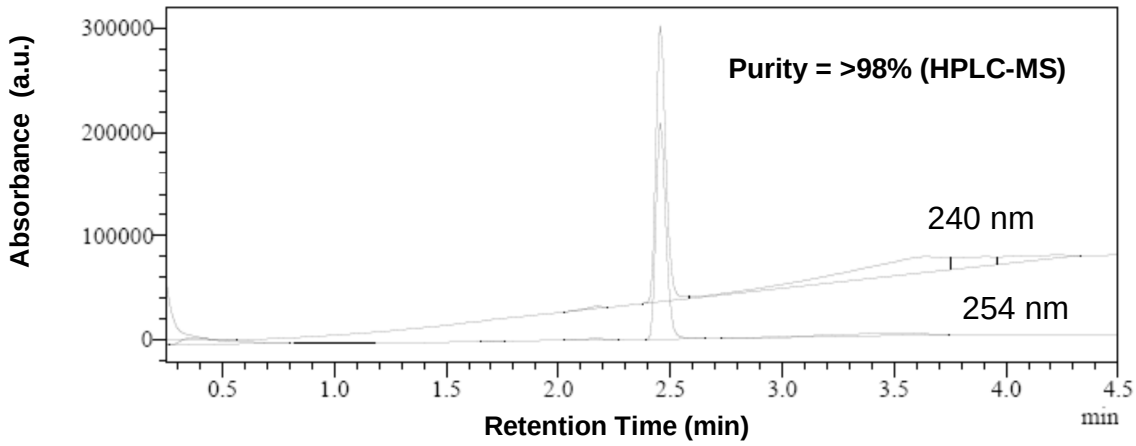

Figure 4c. Positive ion Mass Spectrum of **ML194**

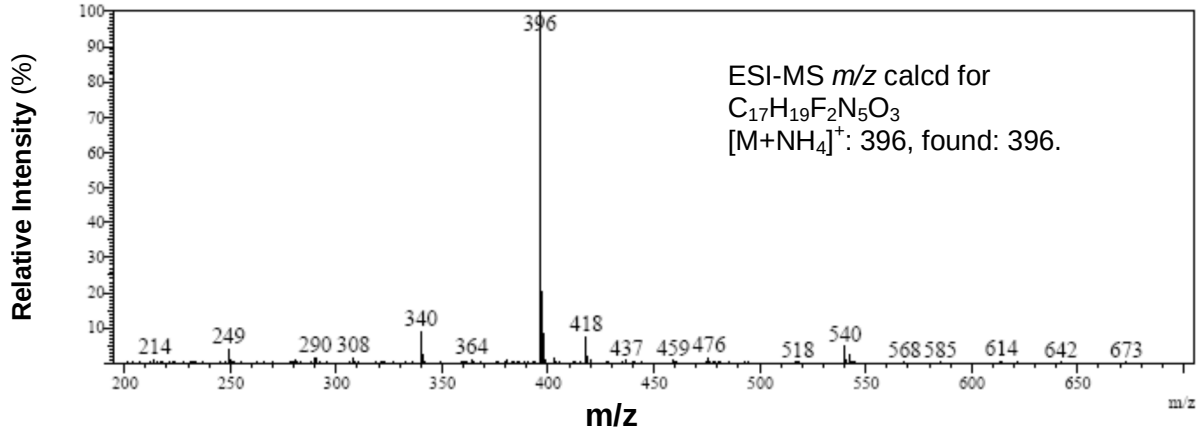

d. PubChem CID(s) (corresponding to the SID)
For Probe #1: PubChem CID9581011 (corresponding to the SID99309109).

e. If available from a vendor, please provide details.
CID9581011 is commercially available from Maybridge CAT # SPB05142

f. **Submission of probe and probe analogs to the MLSMR: Table 4** below summarizes the deposition of samples of the probe **ML194** and 5 probe analogs to the MLSMR.

Table 4. Submission information on Probe 1: CID2286812 and analogs

Probe /Analog	MLS# (DPI)	MLS-(BCCG#)	CID	SID	Source (vendor/ BCCG syn)	Amt (mg)	Date rcv'd by MLSMR
Probe **ML194**	MLS003177459	0300303	9581011	99309109	Maybridge	25	10/18/2010
Analog 1	MLS003177460	300304	9581008	99309106	Maybridge	20	10/18/2010
Analog 2	MLS003177461	0437443	9581010	99309108	Maybridge	20	10/18/2010
Analog 3	MLS003177462	0437444	9581012	99309110	Maybridge	20	10/18/2010
Analog 4	MLS003177463	0437445	9581013	99309111	Maybridge	20	10/18/2010
Analog 5	MLS003177464	0437446	9581015	99309113	Maybridge	20	10/18/2010

g. Describe mode of action for biological activity of probe

Probe **ML194** identified in this project is acting at the beginning of the GPR35 signaling pathway. Ligand binding causes phosphorylation of the GPCR, which in turn causes translocation of the β-arrestin to the membrane, where it binds to the GPCR. The β-arrestin-GPCR complex internalizes into clathrin-coated pits within the cell, where it dissociates and the receptor recycles back to the membrane. Since the assay read-out quantifies formation of β-arrestin-GPCR pits, the identified antagonist interferes with the pit formation or any process upstream. The selectivity of this probe for GPR35 (**Fig. 5**) but not for the related GPR55 orphan receptor in a cognate β-arrestin HCS assay

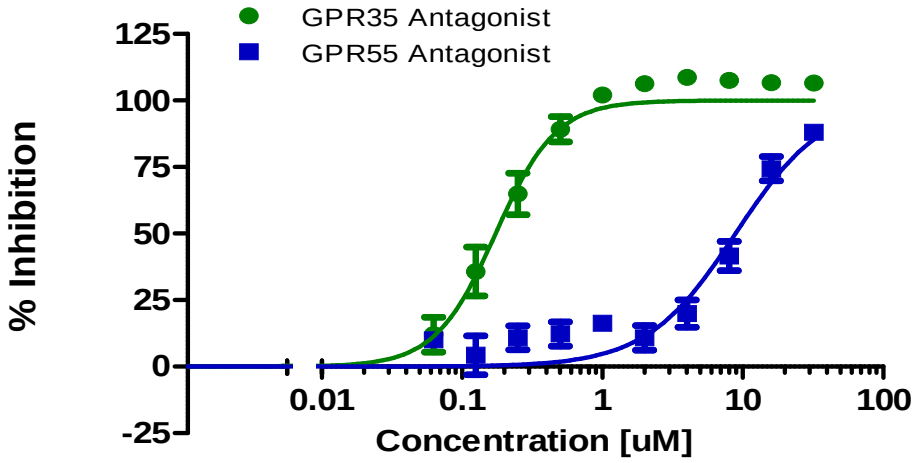

Note:
GPR35 results from 3 independent experiments performed in duplicate
GPR55 results from 2 independent experiments performed in duplicate

Figure 5. Potency & Selectivity of GPR35 Antagonist Probe **ML194**

supports that it is not non-specifically interfering with signaling directly at or downstream of the β-arrestin signaling pathway. An additional secondary assay by Dr. Abood demonstrated that the probes did inhibit Erk1/2 phosphorylation. This confirms that our imaging assay based results translate to the authentic downstream biological response.

h. The synthesis of **ML194** is outlined in Scheme 1 below.

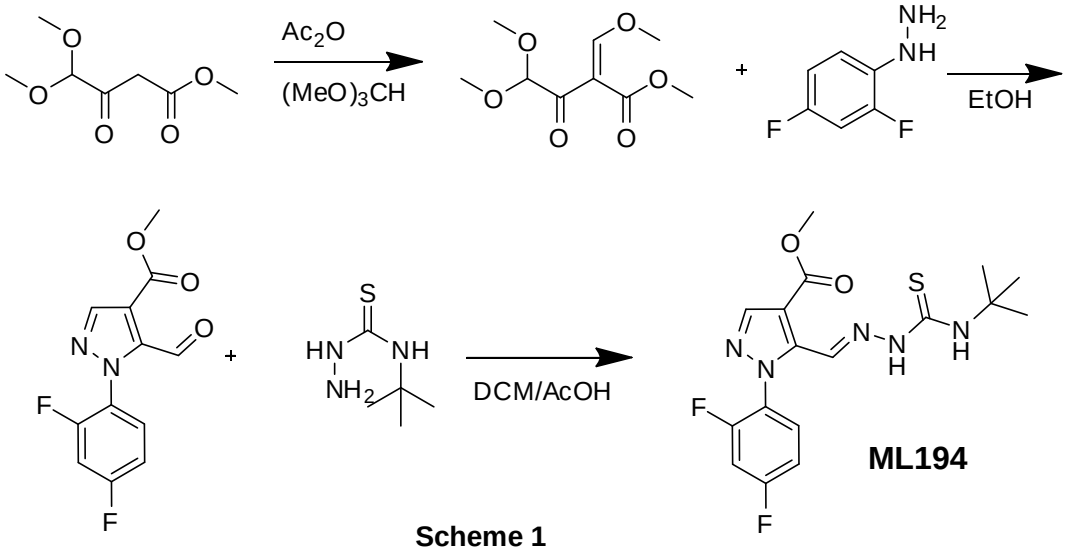

Scheme 1

Methyl 4,4-dimethoxy-3-oxobutanoate was mixed with 1.2 equivalents of acetic anhydride in trimethylorthoformate and the reaction mixture was heated to reflux for 3h. The excess solvents and reagents were removed *in vacuo* and the product methyl 4,4-dimethoxy-2-(methoxymethylene)-3-oxobutanoate was mixed with (2,4-diflurophenyl)hydrazine (1.2 eq.) in anhydrous ethanol at 0°C and slowly warmed to rt. After acidic workup and evaporation of solvents and flash chromatography (ethyl acetate/hexanes), the resultant pyrazole carboxaldehyde was isolated. This product was subsequently treated with *N*-(*tert*-butyl)hydrazinecarbothioamide (1.3 eq) in dichloromethane with 1% acetic acid. The product mixture was purified via reverse-phase HPLC to afford **ML194**.

i. Center summary of probe properties

We have screened the MLSMR library and developed a novel 3rd antagonist probe **ML194** for the GPR35 orphan receptor whose pyrazole core represent a novel chemical scaffold compared to the previous pyrazolo-pyrimidine and the thioxothiazolidinone (rhodanine) based probes, **ML144** and **ML145**, respectively. The structures of these probes and the current probe and their salient properties are shown below. While **ML194** is 8-fold less potent and 19-fold less selective than **ML145**, we still considered it of value as a probe, since it represents a novel chemical scaffold that does not have the potential liabilities of the rhodanine core (a PAINS chemotype) of **ML145** previously noted in the probe report for this probe.

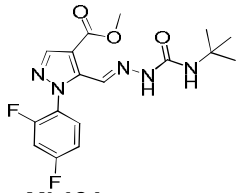

ML194, CID9581011
160 nM GPR35
~9,080 nM GPR55
~57-fold selective

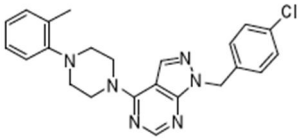

ML144, CID1542103
2.2 µM GPR35
>32 µM GPR55
>15X selective

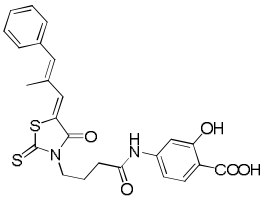

ML145, CID2286812
20.1 nM GPR35
~21,700 nM GPR55
>1,080-fold selective

ML194 does contain a urea moiety via a hydrazone linkage and a methyl ester, though neither seems to be rapidly hydrolyzed in 1:1 PBS/acetonitrile (see "*In vitro stability and solubility* of **ML194**" **Table 5** and paragraph below it). However, **ML194** does represent an improvement over **ML144** in terms of *in vitro cellular* potency (>10-fold) and selectivity (4-fold). While amongst these three probes **ML144** appears most "drug-like", **ML194** (and **ML145**) may still be useful as a tool compound for acute ex vivo tissue slice studies. For *in vivo* work though the very poor microsomal stability presents a challenge.

ML194 Glutathione conjugation assay. To assess the potential of **ML194** for covalent modification, the glutathione transferase activity of the probe compound in the rat hepatic S9 fraction was measured (**Fig. 6a**). The S9-based GSH transferase assay has been shown to be a reliable means of identifying compounds known to react with GSH. Briefly, compounds were incubated at 10 µM in PBS buffer with 2 mg/ml rat hepatic S9 fraction and 10 mM glutathione at 37°C for 1.5 hours. The incubation was stopped by protein precipitation using acetonitrile. After drying down of the supernatant, the residues were reconstituted and analyzed by positive-ion electrospray LCMS and analyzed for the presence of any glutathione conjugates. The LCMS data after 1.5 hours showed 98.4% of unchanged probe compound (**Fig. 6b**, compare peak area at 0 and 90 mins), indicating a low propensity for covalent modification. In addition, none of the expected GSH conjugate masses were detected. The compounds were tested in duplicate along with the positive control diclofenac, a known GSH conjugator, which showed the expected conjugate masses. **ML194** was stable in spite concerns that the hydrazone moiety might be reactive.

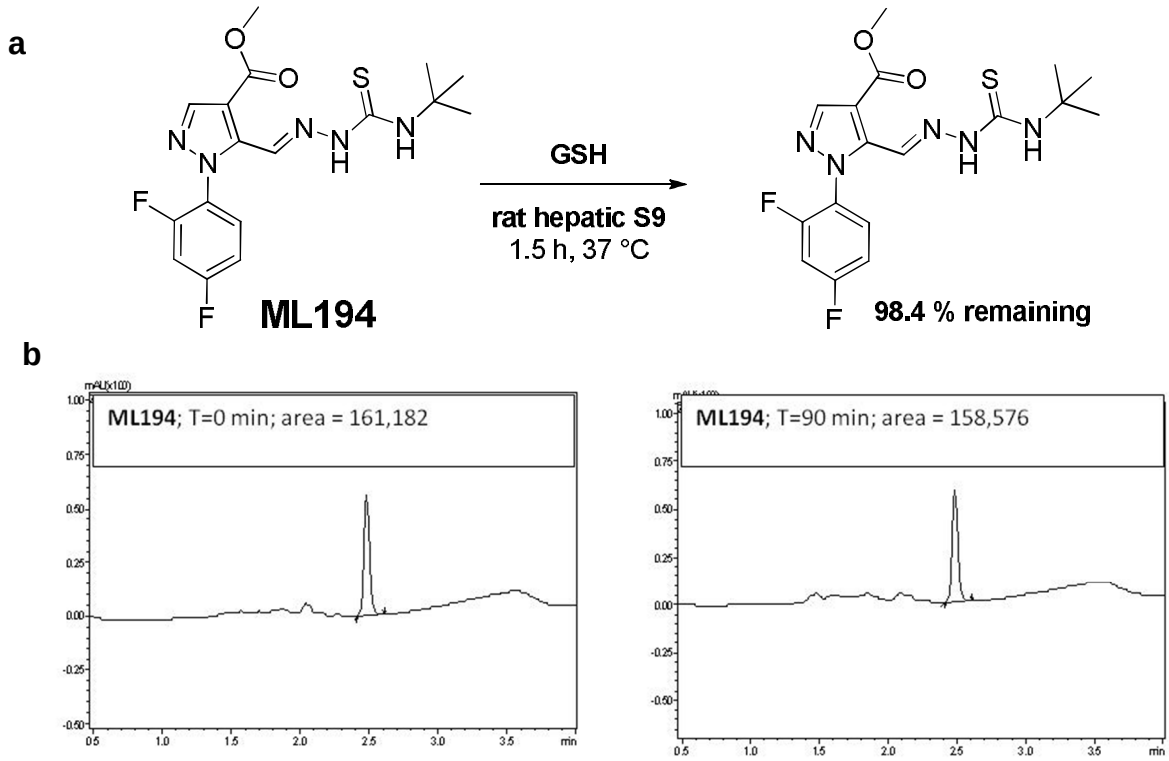

Figure 6. Lack of glutathione reactivity of ML194. (**a**) schematics of S9 incubation -**ML194** was incubated with glutathione and rat S9 fraction for 1.5 hours. (**b**) HPLC-MS analysis showed 98.4% of the parent compound remained after 1.5 hours. Also, no GSH adduct masses were detected.

In Vitro Pharmacology Profiles of Probe **ML194** (CID9581011) were evaluated in a detailed *in vitro* pharmacology screen and the results are shown in **Table 5**. Profiling assays.

Table 5. Summary of *in vitro* ADMET/PK Properties of the GPR35 Antagonist Probe

Probe CID Probe ML# BCCG MLS-#	**Aqueous Solubility** (µg/mL)[a] [*µM*][a] (@ pH) (1XPBS 7.4)	**PAMPA Pe** ($x10^{-6}$ cm/s)[b] (@ pH)	**Plasma Protein Binding (% Bound)**		**Plasma Stability**[c] Human/Mouse 1x PBS, pH 7.4	**Hepatic Microsome Stability**[d] Human/Mouse NADPH minus	**Hepatic Toxicity**[e] LC50 (µM)
			Human 1µM/ 10µM	**Mouse** 1µM/ 10µM			
CID9581011 **ML194** MLS-0300303 m.w. 395.4	0.31 (5.0) 0.51 (6.2) 0.59 (7.4) 0.38 (PBS) *0.78 (5.0)* *1.3 (6.2)1.5 (7.4)* *0.96 (PBS)*	852 (5.0)* 991(6.2)* 586(7.4)*	98.09/ 97.54	97.85/ 98.61	11.28/31.49 2.09/1.42 18.46	0.88/0.65 0.79/44.16	>50

[a] in aqueous buffer (phosphate-free), pH's 5.0/6.2/7.4 or 1X phosphate buffered saline (PBS) pH7.4 (in red font); in µM units in *blue italicized text*
[b] in aqueous buffer (phosphate-free); Donor compartment pH's 5.0/6.2/7.4; Acceptor compartment pH 7.4
[c] % remaining at 3 hr; in Plasma: PBS, (1:1), pH 7.4 (red font); % remaining at 32 hrs in 1X PBS only (in blue font)
[d] % remaining at 1 hr; without NADPH regenerating system (red font)
[e] towards Fa2N-4 immortalized human hepatocytes
*Cmpd was significantly trapped in the membrane

In vitro stability and solubility of **ML194.** The solubility of this probe was poor at all pH's tested in phosphate-free buffer (PBS). Stability of **ML194** was investigated in PBS buffer at room temperature

(**Figure 1**). Initial experiments examining the stability of **ML194** seemed to suggest that the probe degrades rapidly in PBS buffer. However, visual examination of the **ML194** PBS stock solution confirmed that most of the compound was not soluble, so we hypothesized that the apparent "degradation" in PBS was a reflection of time-dependent compound precipitation. We also were unable to detect any of the expected pyrazole aldehyde breakdown products of the hydrazone nor the free acid in a full MS scan. Therefore, we prepared the stock solution of **ML194** in acetonitrile then diluted with 1 part PBS (1:1 PBS/ACN), then repeated the stability analysis. Under these conditions, **ML194** appeared to be *completely stable* with more than 98% remaining after 48 hrs (see **Fig. 7** and **Table 6** below) confirming that confounding poor PBS solubility of **ML194** rather than chemical instability being the culprit. This relatively poor aqueous solubility of **ML194** impacts several of the ADME/T properties to yield apparently poorer values as detailed in the following paragraphs below.

Fig. 7. ML194 Stability in 1:1 PBS/ACN

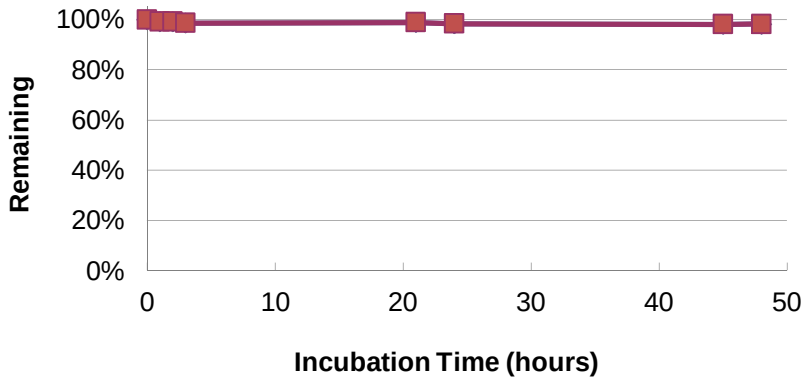

Table 6. Stability of **ML194** in 1:1 PBS/ACN

MLS-0300303	**CID9581011**
Time (hr)	*Remaining*
0	100.0%
1	99.2%
2	99.2%
3	98.6%
21	98.9%
24	98.4%
45	98.1%
48	98.2%

The PAMPA (**P**arallel **A**rtificial **M**embrane **P**ermeability **A**ssay) assay is used as an *in vitro* model of passive, transcellular permeability. An artificial membrane immobilized on a filter is placed between a donor and acceptor compartment. At the start of the test, drug is introduced in the donor compartment. Following the permeation period, the concentration of drug in the donor and acceptor compartments is measured using UV spectroscopy. In this assay **ML194** has a bell-shaped permeability with good permeability at all pHs tested. However, we note that the compound is significantly trapped in the membrane, probably a reflection again of its poor solubility. We have not examined the *in vivo* CNS penetration potential of **ML194** as this would require animal work that is out of scope of the MLPCN and funding.

Plasma Protein Binding is a measure of a drug's efficiency to bind to the proteins within blood plasma. The less bound a drug is, the more efficiently it can traverse cell membranes or diffuse. Highly plasma protein bound drugs are confined to the vascular space, thereby having a relatively low volume of distribution. In contrast, drugs that remain largely unbound in plasma are generally available for distribution to other organs and tissues. **ML194** is highly bound (97.5-98.6%) to both human and mouse plasma.

Plasma Stability is a measure of the stability of small molecules and peptides in plasma and is an important parameter, which strongly can influence the *in vivo* efficacy of a test compound. Drug candidates are exposed in plasma to enzymatic processes (proteinases, esterases), and they can undergo intramolecular rearrangement or bind irreversibly (covalently) to proteins. **ML194** appears to be unstable in human plasma, though much of this apparent instability may be a reflection of its poor solubility and time-dependent precipitation as noted above. This may explain the paradoxically higher **ML194** remaining in whole plasma (11.3% human/31.5% mouse) compared to 1:1

plasma/PBS (2.1% human/1.4% mouse). Dilution of plasma components would be expected to slow degradative processes and lower protein binding, so the apparently lower % remaining is consistent with the notion of compound insolubility and precipitation, leading to underestimation by LC-MS. We also note that while the apparent 18.5% **ML194** remaining after 32 hrs in PBS alone higher that the 1:1 plasma/PBS value, these estimations are suspect due to inherent insolubility in PBS, as noted from the "restored" stability of **ML194** when studied in 1:1 PBS/ACN. We note the duration of the functional GPR35 HCS assay is 1 hr in cell culture media before cell fixation, so most of the effect does come from the parent molecule and little should derive from the expected breakdown products (**ML194** acid form from methyl ester hydrolysis or the aldehyde if the hydrazone is cleaved).

The microsomal stability assay is commonly used to rank compounds according to their metabolic stability. This assay addresses the pharmacologic question of how long the parent compound will remain circulating in plasma within the body. **ML194** shows poor stability in both human and mouse liver homogenates in the presence of absence of NADPH co-factor.

ML194 shows no toxicity (>50 μM) toward human hepatocyctes.

j. A tabular presentation summarizing known probe properties

Table 7. Properties **ML194** (CID9581011) MLS-0300303

Calculated Property	**Value**
Molecular Weight [g/mol]	395.426866
Molecular Formula	$C_{17}H_{19}F_2N_5O_2S$
XLogP3-AA	2.9
H-Bond Donor	2
H-Bond Acceptor	6
Rotatable Bond Count	6
Tautomer Count	9
Exact Mass	395.122752
MonoIsotopic Mass	395.122752
Topological Polar Surface Area	113
Heavy Atom Count	27
Formal Charge	0
Complexity	572
Isotope Atom Count	0
Defined Atom StereoCenter Count	0
Undefined Atom StereoCenter Count	0
Defined Bond StereoCenter Count	1
Undefined Bond StereoCenter Count	0
Covalently-Bonded Unit Count	1

5. Comparative data showing probe specificity for target in biologically relevant assays

ML194 is a novel 3rd antagonist probe for the GPR35 orphan receptor whose pyrazole core represent a novel chemical scaffold compared to the previous pyrazolo-pyrimidine and the thioxothiazolidinone (rhodanine) based probes, **ML144** and **ML145**, respectively. Further follow-up work has been conducted in the laboratories of Dr. Barak and collaborator (Dr. Abood) as outlined in the Chemical Probe Development Plan (CPDP) as post Probe Nomination characterization. The additional downstream assay is as described below and the SAR data summarized for the probe series (**Table 8**)

Assay for ERK1/2 Activity in GPR35-Overexpressing U2OS Cells [GI: 33695097; Gene: 2859]: Assay performed by Dr. Abood's laboratory characterizes the downstream ERK phosphorylation activity of probe compounds. This is an "in-cell" Western assay which utilizes a cell line permanently expressing a beta-arrestin GFP biosensor and human GPR35 receptor. Upon agonist-mediated GPCR activation by EC80 Zaprinast, ERK1/2 phosphorylation occurs as measured by pERK1/2

antibodies (see AID 463217 for details and Supplemental Materials below). The ERK1/2 assay is generally much less sensitive than the beta-arrestin GPCR assays and the assay protocol does not allow for compound pre-incubation before agonist addition, which may result in much higher IC50 values (up to 10-fold) for the pERK-ICW potencies as compared the GPR35 assay (12). This can be seen in **Table 8** where the nanomolar GPR35 probe and analogs yield micromolar potency in ERK phosphorylation. We note that while there are some rank order differences in the apparent pERK IC50s versus the GPR35 IC50s, possibly due different solubility or ADME properties, the overall conclusion is that the probe scaffold class does have measureable activity in the downstream assay on the authentic signaling pathway.

Table 8. Comparative Downstream assays by Assay Provider for CID9581011

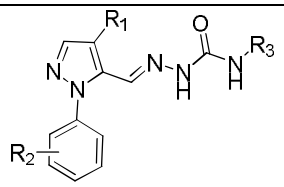					**GPR35** *AID 463227*	**pERK-ICW**	
CID	**SID**	**R1**	**R2**	**R3**	**IC50 (μM)**	**IC50 (μM)**	**n**
9581011	99309109	COOMe	2,4-di-F	tBu	0.160	1.4±0.09	6
9581010	99309108	COOMe	2,4-di-F	4-Cl-Ph	0.171	1.7±0.17	6
9581015	99309113	COOMe	4-Cl	Ph	0.211	21.8±0.10	6
9581013	99309111	COOMe	4-Cl	Me	1.25	4.1±0.11	6
9581008	99309106	COOMe	2,4-di-F	Me	2.49	2.29±0.9	6

ML194 has been submitted for profiling to the NIMH Psychoactive Drug Screening Program (PDSP) in Dr. Bryan Roth's laboratory at University of North Carolina at Chapel Hill.

6. Future studies

GPR35 is emerging as an important target in pain (spinal antinociception as well as inflammatory pain), heart disease, asthma, inflammatory bowel disease and cancer, areas with unmet medical needs. These probes have only been evaluated in cellular HCS assays, and we have no guidance of any CNS penetration and effective exposure levels (vs. the *in vitro* IC50), so additional studies and limited compound scale-up would need to be planned and funded. There are five recently recognized areas to which GPR35 signaling may play an important role, metabolic disease (diabetes), hypertension, asthma, pain, and inflammatory bowel disease (IBD), (see review G. Milligan, Orthologue selectivity and ligand bias: translating the pharmacology of GPR35 see TIPS-858 in press). Each of these areas alone is medically important and each would benefit by the use of GPR35 antagonists to further studies in their respective animals models. Moreover, the occurrence of GPR35 receptors outside the CNS also suggests less stringent requirements for the chemical optimization of GPR35 antagonist compounds because a subclass of their medically relevant targets has greater accessibility. In this regard, in addition to our use of GPR35 ligands in visceral pain models (Zhao *et al*.), we (Barak & Abood) are currently collaborating in preliminary studies on the role of GPR35 ligands in an IBD model; and the ability to obtain more defined physiological data as well as outside financial support would certainly benefit from improved GPR35 antagonists with better pharmacological properties. The current probes are useful for cell based and in vitro studies, but would benefit from additional SAR development and compound optimization of some of the ADME/T properties such as solubility and protein binding, which would also influence the apparent plasma concentration or activity. Other additional studies to delineate whether **ML194** acts on the GPCR-dependent or the non GPCR-dependent path via direct β-arresting signaling are also contemplated and can be undertaken using the high affinity GPR35 ligand pamoic acid that we

discovered (Zhao *et al.*) in conjunction with the antagonists developed as a consequence of this proposal.

7. References:

1. O'Dowd BF, Nguyen T, Marchese A, Cheng R, Lynch KR, Heng HH, Kolakowski LF, Jr. and George SR (1998) Discovery of three novel G-protein-coupled receptor genes. *Genomics* **47**:310-3.
2. Guo J, Williams DJ, Puhl HL, 3rd and Ikeda SR (2008) Inhibition of N-type calcium channels by activation of GPR35, an orphan receptor, heterologously expressed in rat sympathetic neurons. *J Pharmacol Exp Ther* **324**:342-51.
3. Johns DG, Behm DJ, Walker DJ, Ao Z, Shapland EM, Daniels DA, Riddick M, Dowell S, Staton PC, Green P, Shabon U, Bao W, Aiyar N, Yue TL, Brown AJ, Morrison AD and Douglas SA (2007) The novel endocannabinoid receptor GPR55 is activated by atypical cannabinoids but does not mediate their vasodilator effects. *Br J Pharmacol* **152**:825-31.
4. Ryberg E, Larsson N, Sjogren S, Hjorth S, Hermansson NO, Leonova J, Elebring T, Nilsson K, Drmota T and Greasley PJ (2007) The orphan receptor GPR55 is a novel cannabinoid receptor. *Br J Pharmacol* **152**:1092-101.
5. Taniguchi Y, Tonai-Kachi H and Shinjo K (2006) Zaprinast, a well-known cyclic guanosine monophosphate-specific phosphodiesterase inhibitor, is an agonist for GPR35. *FEBS Lett* **580**:5003-8.
6. Brown AJ (2007). Novel cannabinoid receptors. *Br J Pharmacol* **152**:567-75.
7. Ohshiro H, Tonai-Kachi H and Ichikawa K (2008) GPR35 is a functional receptor in rat dorsal root ganglion neurons. *Biochem Biophys Res Commun* **365**:344-8.
8. Okumura S, Baba H, Kumada T, Nanmoku K, Nakajima H, Nakane Y, Hioki K and Ikenaka K (2004) Cloning of a G-protein-coupled receptor that shows an activity to transform NIH3T3 cells and is expressed in gastric cancer cells. *Cancer Sci* **95**:131-5.
9. Shrimpton AE, Braddock BR, Thomson LL, Stein CK and Hoo JJ (2004) Molecular delineation of deletions on 2q37.3 in three cases with an Albright hereditary osteodystrophy-like phenotype. *Clin Genet* **66**:537-44.
10. Barak LS, Ferguson SS, Zhang J, Martenson C, Meyer T and Caron MG (1997) Internal trafficking and surface mobility of a functionally intact beta2-adrenergic receptor-green fluorescent protein conjugate. *Mol Pharmacol* **51**:177-84.
11. Baell B J, Holloway AG (2010) New Substructure Filters for Removal of Pan Assay Interference Compounds (PAINS) from Screening Libraries and for Their Exclusion in Bioassays. *J Med Chem*. 2010 Feb 4. [Epub ahead of print]. PMID: 20131845 [PubMed - as supplied by publisher]
12. Zhao P, Sharir H, Kapur A, Cowan A, Geller EB, Adler MW, Seltzman HH, Reggio PH, Heynen-Genel S, Sauer M, Chung TD, Bai Y, Chen W, Caron MG, Barak LS, Abood ME. Targeting of the orphan receptor GPR35 by pamoic acid: a potent activator of extracellular signal-regulated kinase and β-arrestin2 with antinociceptive activity (2010) Mol Pharmacol. Oct;78(4):560-8.

Supplementary Materials:

Assay for ERK1/2 Activity in GPR35-Overexpressing U2OS Cells

Data Source: Dr. Mary Abood, Dr. Pingwei Zhao
Source Affiliation: Temple University
Network: NIH Molecular Libraries Probe Production Centers Network (MLPCN)
Grant Proposal Number: 1X01MH085708-01
Assay Provider: Dr. Lawrence Barak, Duke University

The aim of this assay is to characterize downstream ERK phosphorylation activity of compounds originally identified in "Image-based HTS for Selective Antagonists of GPR35" (AID 2058). Compounds were either acquired from commercial sources or synthesized by the Sanford-Burnham Center for Chemical Genomics.

This On-Cell Western assay utilizes a cell line permanently expressing a beta-arrestin GFP biosensor and human GPR35 receptor. Upon agonist-mediated GPCR activation, ERK1/2 phosphorylation occurs as measured by pERK1/2 antibodies.

GI: 33695097
Gene: 2859
GPR 35, G-Protein Coupled Receptor 35

Protocol:

Assay Materials:
1) 96-well plates (FALCON 353075)
2) U2OS (Human Osteosarcoma) cell line stably expressing the Beta-arrestin GFP and human GPR35 receptor
3) Culture Media: DMEM with 10% Fetal Bovine Serum and selection antibiotics - 200ug/ml G418 and 100ug/ml Zeocin
4) EC80 concentration of Agonist: 10 µM Zaprinast
5) DMSO solution
6) Test compounds Working Solution: 10mM Stock in 100% DMSO, diluted in assay buffer (HBSS Cellgro #21-023-CV)
7) Fixative Solution: 4% Paraformaldehyde (PFA) diluted in PBS
8) Permeabilization Solution: 0.1% Triton X-100 in PBS
9) Primary phosphor-ERK1/2 antibody (Cell Signaling Technology, diluted 1:100)
10) Goat anti-rabbit 800CW secondary antibody diluted 1:800 in Licor blocking buffer together with Sapphire700 (diluted 1:1000) and DRAQ5 (diluted 1:2000) for normalization purpose

Assay Procedure:
1) Cells were grown to confluence in 96-well plates and serum-starved overnight prior to assay.
2) Prior to drug treatment cells were washed once with HBSS at room temperature.
3) Compounds were added at varying dose response concentrations together with the agonist (10µM Zaprinast) to compound and negative control wells.
4) DMSO only was added to wells for a final concentration of 0.1%.
5) Plates were incubated for 15 minutes at room temperature.
6) Media was aspirated from all wells.
7) Fixative solution was added to each well for a final concentration of 4% PFA and plates were incubated for 60 minutes at room temperature.
8) Fixative was aspirated and cells were permeabilized with 0.1% Trion X-100 in PBS for 5 washes at 10 minutes per wash.
9) LI-COR blocking buffer was added and samples were shaken on a rotator for 1 hour.
10) Primary antibodies were applied for overnight at 4 degree C with rotation, followed by washing 4 times for 5 minutes each in PBS+ 0.1% Tween-20 with gentle shaking at RT.
11) Cells were incubated with secondary antibodies for 2 hours at room temperature. Sapphire700 and DRAQ5 solutions were added together with the secondary antibodies for normalization. Plates were protected from light.

12) Membranes were washed 4 times for 5 minutes each in PBS + 0.1% Tween-20 with gentle shaking at RT, and were protected from light.
13) Plates were dried and scanned using a LI-COR Odyssey Infrared Imager.
14) IC50 values were calculated employing a sigmoidal dose-response equation through non-linear regression in Prism 4.0 software.

Definition of Active Compound:
Compounds with IC50 < 10 μM were considered active.